Some Remarks on Heat Flow and Gravity Anomalies[1]

DAN P. MCKENZIE

Seismological Laboratory, California Institute of Technology
Pasadena, California 91109

Heat flow anomalies on the oceanic ridges and the large free air gravity anomalies observed from the earth's surface and from satellites are often believed to be surface expressions of high temperatures and flow within the mantle. A simple model for the temperature within a spreading sea floor can, however, reproduce the shape and magnitude of the observed anomalies. Thus, it is not necessary for the upper mantle to be hotter beneath ridges than it is elsewhere. A similar model may be used to relate the free air gravity anomaly to the stress in the lithosphere. The results show that long-wavelength harmonics of the external gravity field cannot be supported by the strength of the lithosphere. Most free air anomalies observed on the surface can be maintained in this way, except possibly the largest of those over the trenches.

INTRODUCTION

The present interest in sea floor spreading and continental drift has emphasized how little is known about the motion in three dimensions within the mantle. It is important, therefore, to extract as much information as possible from the conventional geophysical measurements (viz., measurements of gravity and oceanic heat flow) until some hypothesis as powerful as that of *Vine and Matthews* [1963] as suggested for examining flow at depth. It is the principal purpose of this paper to demonstrate that both gravity and oceanic heat flow are probably controlled by the strength and thermal properties of the crust and uppermost mantle, or what is often called the lithosphere. The same is not true of the long-wavelength harmonics of the gravity field determined from the motion of satellites, which are not affected by the lithosphere and may well be related to flow patterns within the mantle. This is essentially what *Runcorn* [1965] has suggested, though his analysis of the convection problem is undoubtedly too simple.

Any discussion of the significance of gravity and heat flow observations requires some mechanical and thermal model for the crust and upper mantel. At low temperatures (less than ~700°C) the mechanical behavior of hard high-melting-point minerals, like olivine, is principally elastic until the yield stress is reached, and then the material fails by brittle fracture. At higher temperatures various diffusion-controlled processes permit minerals to creep at all stresses [*McKenzie*, 1967*a*], and therefore any stress deep within the mantle must be maintained by some active process against dissipation by creep. These remarks suggest that the outer perhaps 50–100 km of the earth must behave as a rigid layer and that the places where this is not true will be marked by shallow earthquakes. Such a model is by no means new; it was originally suggested in the nineteenth century to explain isostatically compensated mountain ranges [see, for instance, *Fisher*, 1889]. As the sea floor spreads, the lithosphere must move as a solid layer and carry the magnetic anomalies with it. Though continental drift and regional tectonics are presumably the surface expressions of mantle movements, it is not obvious what other geophysical observations are relevant. The principal reason for this ignorance is that the lithosphere strongly modifies the stress and temperature fields as it transmits them from its lower boundary to the earth's surface. The strength and long thermal decay time (~10 million years) of the lithosphere prevent the use of simple corrections, but it is still possible to separate observations into two groups, according to whether or not they are dominated by the properties of the lithosphere.

The early measurements of heat flow at sea

[1] Contribution 1474, Division of Geological Sciences, California Institute of Technology, Pasadena.

[*Bullard*, 1954; *Bullard et al.*, 1956] showed that high values were common on the mid-Atlantic ridge. Many measurements have since been made, and the average heat flow through the ridges in the Atlantic, east Pacific, and Indian oceans is considerably above the oceanic mean [*Lee and Uyeda*, 1965; Figures 2–4]. These anomalies are larger and more consistent than any others in the heat flow field. Two explanations have been suggested. The first produces the high flow by intrusion of hot basalt and peridotite in dykes along the axis of ridge. As the sea floor spreads away from the ridge, the hot rock slowly cools. This idea suggests that the width of the anomaly should be controlled by the spreading rate. If this theory is correct, the high heat flow is a result of tension in the lithosphere and is not the surface expression of temperature anomalies in the upper mantle.

The other suggestion ignores the lithosphere and produces the high heat flow by narrow upwelling limbs of convection cells, which are required to be beneath the axes of the ridges. *Turcotte and Oxburgh* [1967] have used boundary layer theory to analyze this idea and have neglected the variation of viscosity with temperature. The difference between the two suggestions is in the nature of the boundary layer, since their equation 18 and surface boundary conditions are identical to those used here. The lithosphere is a mechanical layer produced by the rapid variation of creep rate with temperature; its existence does not depend on a high Rayleigh number. The thermal boundary layer required by the second hypothesis is governed by the convection process and, hence, relates the surface observations directly to flow in the mantle. The origin of the anomaly is convective in both cases, since the intrusion of basalt and peridotite is driven by thermal bouyancy forces. If the first hypothesis is correct, the heat flow anomaly is a consequence of sea floor spreading and cannot be used to examine the temperature distribution in the mantle. The anomaly should follow the axis of the ridge and be offset by transform faults, as *Vacquier and Von Herzen* [1964] believe it is in the equatorial Atlantic. With this hypothesis, however, there is no reason to suppose that the axis of the mantle convection cell is offset in the same manner.

A simple model for a spreading sea floor is a slab of constant thickness moving with a constant velocity (Figure 1). The complicated intrusion mechanisms by which the sea floor is produced along a mid-ocean ridge are neglected. Instead, the slab is produced at $x = 0$ at constant temperature. Though this boundary condition is certainly unrealistic, the agreement between the heat flow anomaly from this model and the anomaly from the model used by *Langseth et al.* [1966] shows that, except in the

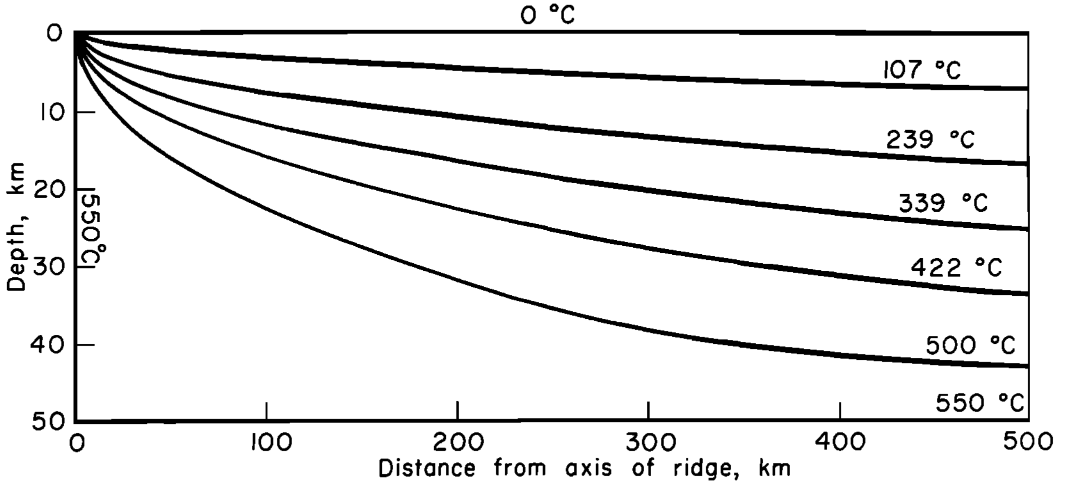

Fig. 1. Isotherms within the layer spreading at 4 cm/yr to the right. This model produces the theoretical heat flow in Figure 4 and has $\mathcal{R}$ = 27.6, ×4 vertical exaggeration.

central region, the shape and size of the anomaly are little affected by the details of the intrusion. If the thickness of the lithosphere is taken to be 50 km, there is good agreement with the observed width and shape of the ridge anomalies (Figure 2–4). The difference between this conclusion and that of Langseth et al. is caused by the difference in thickness of the spreading layer. In the model used here the temperature is constant at and below 50 km, and therefore horizontal isotherms below this depth are not in conflict with the surface heat flow. Clearly, this model is not the only possible one, and a choice between it and the model of Turcotte and Oxburgh cannot be made on the basis of heat flow observations alone. Since only the thickness of the lithosphere is variable, however, the model used here is probably the simplest that can account for the observations and that does not involve any assumptions about the Rayleigh number within the mantle.

Large long-wavelength gravity anomalies may be caused by surface distortions and density anomalies produced by flow in the mantle. Many small short-wavelength anomalies are, however, produced by surface topography and density variations within the crust and uppermost mantle. As *Fisher and Hess* [1962] have pointed out, a mantle origin is required only for the anomalies that cannot be supported by the strength of the lithosphere. In the absence of elastic and viscous stresses, the gravity field of the earth would be that of a rotating hydro-

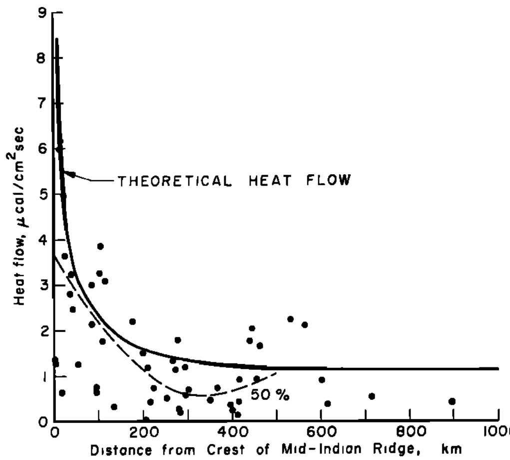

Fig. 3. Heat flow in the Indian Ocean.

static liquid, and therefore any gravity anomalies (including those produced by surface topography) must be supported by an internal stress field. This argument suggests the stress field should be estimated from the free air anomaly observed on an equipotential in order to decide whether a mantle origin is required. The Bouguer and isostatic anomalies are not suitable because various assumptions are required in their calculation and also because the topographic anomaly has been removed. Most gravity surveys are made to discover the density distribution beneath the surface, when topography is a troublesome correction. If, however, it is the stress field that is of interest, an

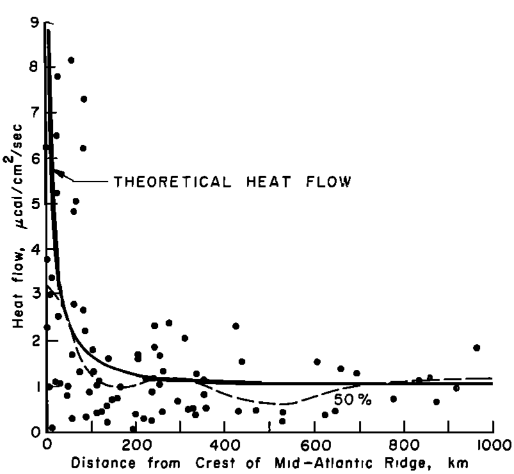

Fig. 2. Heat flow in the Atlantic Ocean.

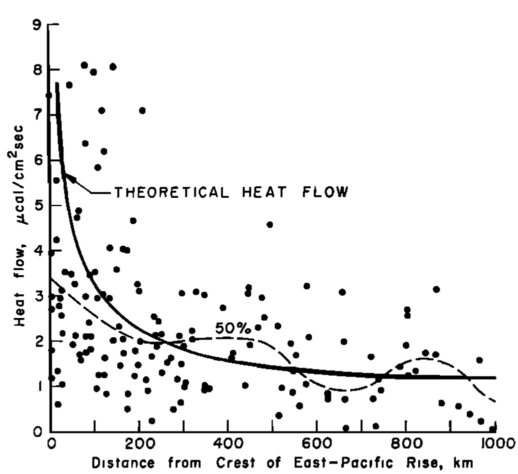

Fig. 4. Heat flow in the Pacific Ocean.

anomaly produced by the air-rock or sea-rock interface is just as important as one produced by the topography of the M discontinuity.

The model used here (Figure 5) to estimate the stresses required by any anomaly assumes that the anomaly is produced by the topography of the upper surface of the lithosphere. This is probably a good approximation to the trenches, since *Talwani et al.* [1959] have fitted the gravity observations over the Puerto Rico trench with a constant upper mantle density. This model is static and, therefore, is only concerned with the forces that maintain the anomalies and not with the forces that produced them. Though the stress field within the elastic layer cannot be determined uniquely, an estimate of the minimum value consistent with the amplitude and wavelength of the gravity anomaly may be obtained. *Jeffreys* [1929] discusses isostasy with a similar model by giving the normal load on the upper surface and then determining the compensation. Any such isostatic compensation is impossible in the model used here, because the deformation, not the load, is given as a boundary condition. Though there are more assumptions in this model than in the model for the heat flow, the results do suggest that a shear strength of a few hundred bars throughout the lithosphere can maintain the free air gravity anomalies observed at the earth's surface. The strength of the lithosphere, however, is quite unable to support the long-wavelength anomalies required to explain the motion of satellites. These remarks do not imply that the trenches are not the sites of down-going limbs of convection cells; they merely suggest that the gravity anomalies need not be maintained by normal stresses and density variations resulting from such flow.

Heat Flow

The general equation for the temperature within a moving material when dissipation is absent is

$$\rho C_P\left[\frac{\partial T}{\partial t} + \mathbf{v}\cdot\nabla T\right] = \kappa\nabla^2 T + H \qquad (1)$$

where $\mathbf{v}$ is the velocity of the material, κ is the thermal conductivity, and H is the rate of internal heat generation. Many methods can be used to solve this equation when $\mathbf{v} = 0$, but there are also a few special cases when exact solutions can be obtained with $\mathbf{v} \neq 0$. If

$$\mathbf{v} = (v, 0, 0) \qquad (2)$$

where v is constant and if z is measured vertically, then in two dimensions (1) becomes

$$\rho C_P\left[\frac{\partial T}{\partial t} + v\frac{\partial T}{\partial x}\right] = \kappa\left[\frac{\partial^2 T}{\partial x^2} + \frac{\partial^2 T}{\partial z^2}\right] + H \qquad (3)$$

Equation 3 is a linear partial differential equation that can be solved in the usual way by separation of variables. The resulting solutions for the x dependence of the eigenfunctions are not orthogonal, however, and therefore only simple boundary conditions on z = constant, the upper and lower surfaces, can be satisfied. The boundary conditions chosen here are that the temperature should be constant on both. This restriction does not apply to the boundary $x = 0$, since the z solutions are orthogonal. Though the complete solution to (3) can be obtained, $\partial T/\partial t$ and H are neglected throughout this discussion. Though both values are probably small, they are omitted to simplify the expression, rather than because their neglect can be rigorously justified. If the thickness of the spreading layer is l and the upper and lower surface temperatures are T_0 and T_1, respectively, substitution of

$$T = (T_1 - T_0)T' + T_0$$
$$x = lx'$$
$$z = lz'$$

into (3) gives

$$\frac{\partial^2 T'}{\partial x'^2} - 2\mathcal{R}\frac{\partial T'}{\partial x'} + \frac{\partial^2 T'}{\partial z'^2} = 0 \qquad (4)$$

where $\mathcal{R}$ is the Rayleigh number for this problem:

$$\mathcal{R} = \frac{\rho C_P v l}{2\kappa} \qquad (5)$$

Thus, the solution for T' is of the form

$$T' = T'(x', z', \mathcal{R}) \qquad (6)$$

The surface heat flow is given by a similar expression:

$$\left(\frac{dT'}{dz'}\right)_{z'=1} = F(x', \mathcal{R}) \qquad (7)$$

Thus, the real half-width of the heat flow anomaly determines $lf(\mathcal{R})$, and therefore any half-width can be obtained from this model by varying l [see *Langseth et al.*, 1966]. A suitable particular integral to (4) is

$$T' = 1 - z' \tag{8}$$

Also

$$A_n \exp(-\alpha_n x') \sin k_n z' \tag{9}$$

satisfies (4) if

$$\alpha_n = \mathcal{R} - \sqrt{\mathcal{R}^2 + k_n^2} \tag{10}$$

The other solution for α_n is positive and therefore must be excluded. The boundary conditions on $z' = 0$ and 1 are satisfied if

$$k_n = n\pi \tag{11}$$

Thus,

$$T' = 1 - z' + \sum_{n=1}^{\infty} A_n \cdot \exp[(\mathcal{R} - \sqrt{\mathcal{R}^2 + n^2\pi^2})x'] \sin n\pi z' \tag{12}$$

A_n may be determined from the temperature on $x' = 0$, which is taken to be the same as that of the lower surface, $T = T_1$ or $T' = 1$:

$$A_n = 2\int_0^1 z' \sin \pi n z' \, dz' = \frac{2(-1)^{n+1}}{n\pi} \tag{13}$$

Then

$$T' = 1 - z' - \sum_{n=1}^{\infty} \frac{2(-1)^n}{n\pi} \cdot \exp[(\mathcal{R} - \sqrt{\mathcal{R}^2 + n^2\pi^2})x'] \sin n\pi z' \tag{14}$$

and

$$-\left(\frac{dT'}{dz'}\right)_{z'=1} = 1 + 2 \cdot \sum_{n=1}^{\infty} \exp[(\mathcal{R} - \sqrt{\mathcal{R}^2 + n^2\pi^2})x'] \tag{15}$$

In general, the isotherms and heat flow may be obtained numerically from (14) and (15) to any desired accuracy. Fortunately, an approximate expression to (15) is sufficient for many purposes. This approximation can be obtained by neglecting all terms in the sum except $n = 1$, and it is valid when x' is large:

$$-\left(\frac{dT'}{dz'}\right)_{z'=1} \simeq 1 + 2 \cdot \exp[(\mathcal{R} - \sqrt{\mathcal{R}^2 + \pi^2})x'] \tag{16}$$

Since $\mathcal{R}^2 \gg \pi^2$ in all the models considered here, (16) can be written

$$-\left(\frac{dT'}{dz'}\right)_{z'=1} \simeq 1 + 2 \exp\left(-\frac{\pi^2 x'}{2\mathcal{R}}\right) \tag{17}$$

If the half-width δ' of the heat flow anomaly is chosen to be that value of x' that gives $-(dT'/dz')_{z'=1} = 2$, then

$$\delta' \simeq \frac{2\mathcal{R} \log_e 2}{\pi^2} \tag{18}$$

or the real half-width δ is

$$\delta \simeq \frac{\rho C_P l^2 v \log_e 2}{\kappa\pi^2} \tag{19}$$

A similar expression can be obtained by a different and less rigorous argument. The time taken before the surface of the spreading layer 'feels' the lower boundary condition is $\sim\rho C_P l^2/\pi^2\kappa$. In this time the layer has moved a horizontal distance $\sim\rho C_P l^2 v/\pi^2\kappa$, which approximately agrees with (19). If this anomaly is to account for the ridge anomalies,

$$\frac{\delta}{v} \simeq \frac{\rho C_P l^2 \log_e 2}{\kappa\pi^2} = C \tag{20}$$

where C is a constant for all ridges. δ can be obtained from *Lee and Uyeda*'s [1965] 50% lines, and v from *Vine*'s [1966] discussion of the magnetic lineations. For the Atlantic ridge, $\delta = 60$ km, $v = 1$ cm/yr, $C = 1.8 \times 10^{14}$; for the Indian, $\delta = 110$ km, $v = 1.5$ cm/yr, $C = 2.2 \times 10^{14}$; and for the East Pacific rise, $\delta = 220$ km, $v = 4.4$ cm/yr, $C = 1.4 \times 10^{14}$. This variation of C is probably not significant, since neither δ nor v are at present well determined. Substitution of

$$\rho = 3.0 \text{ g/cc} \qquad C_P = 0.25 \text{ cal/g °C}$$
$$\kappa = 0.01 \text{ cal/°C cm sec} \qquad C = 1.8 \times 10^{14} \tag{21}$$

into (20) gives $l = 59$ km. For simplicity l is taken to be 50 km ($C = 1.3 \times 10^{14}$) throughout the rest of this section.

In Figures 2, 3, and 4 the heat flow obtained from (15) is superimposed on the diagrams from *Lee and Uyeda* [1965]. The spreading rates used to obtain $\mathcal{R}$ are 1, 2, and 4 cm/yr for the Atlantic, Indian, and East Pacific rises, respectively. The other parameters are the same as above. The agreement with observation is good except perhaps within 50 km of the ridge axes. In this region the heat flow may well be controlled by the details of the intrusion mechanism, which is certainly more complicated than that used in the model. The 50% line for the heat flow through all the ocean basins is about at 1.1 μcal/cm^2 sec. This value requires a temperature of 550°C at a depth of 50 km if the conductivity is that given in (21).

It is surprising that the model agrees well with observations when $x \gg \delta$, since it is in this region that the heat flow is strongly affected by the lower boundary condition. If the temperature gradient were required to be constant as $z \rightarrow -\infty$, rather than $T = T_1$ on $z = 0$, the heat flow would continue to decrease when $x \gg \delta$ as x increased. The agreement therefore suggests that the conductivity may increase markedly at a depth of about 50 km. *Ewing et al.* [1962] have suggested a model for V_S to account for the propagation of surface waves across the Pacific basin with the upper surface of the low-velocity layer at a depth of 55 km. The basaltic magma that is erupted in Hawaii is also believed to come from a depth of about 60 km [*Eaton*, 1962]. Since it is unlikely that any of these values are determined to better than perhaps 10 km, the success of the model could be explained by a high effective conductivity of the low-velocity zone, and this, in turn, could be produced by convection of basaltic magma through a lattice of olivine crystals. This mechanism of heat transfer has recently been discussed by *Elder* [1965]. Provided that the olivine crystals remain in contact with each other, they will dominate the long-term mechanical properties of the region.

If this hypothesis is correct, the temperature gradient in the low-velocity layer must be close to the adiabatic, perhaps 1°C/km, and therefore the upper surface of the low-velocity layer is approximately an isotherm. The equality of the continental and oceanic average heat flow could then be explained if the upper surface of the low-velocity zone were deeper than 50 km beneath continents. There is some evidence from surface waves [*Knopoff et al.*, 1966] and from body waves (C. B. Archambeau, E. A. Flinn, and D. G. Lambert, 'The fine structure of the upper mantle,' in preparation, 1967) that this is the case. Also, under shield areas the low-velocity layer is much reduced, and there are now several measurements of low heat flow in the same regions.

It is possible to produce a model for a trench by substituting $v = -v$, and $T = T_0$ on $x = 0$. There is no reason, however, to believe that the flow is symmetric on each side of the trench, and therefore the results from such a model are unlikely to resemble the observations.

Gravity Anomalies

The largest free air gravity anomalies on the earth's surface occur over trenches and island arcs. Though the density variations that produce them are probably not within the mantle, the supporting stresses must either be maintained by the finite strength of the lithosphere or be produced by flow in the mantle. The first explanation is examined with a simple model to decide whether a reasonable thickness and strength for the lithosphere can account for the observations. The argument against the second hypothesis is the same as that used in the last section; it should not be considered until the first argument has been shown to be insufficient.

Figure 5 shows the two-dimensional model used in this section. Discussion of a three-dimensional model is, fortunately, not necessary because both trenches and ridges are generally linear features. The harmonic distortion of the upper and lower surfaces of the elastic incompressible layer is supported by a stress field within it. The layer floats on an inviscid incompressible liquid half-space of the same density. The boundary conditions on the stress are that the traction vanishes on the upper and lower surfaces of the layer, and that the normal stress is zero on the upper and equal to the fluid pressure on the lower. The variation in gravity may easily be obtained from the continuity of the gravitational potential U and of ∇U on the deformed surface and is entirely a topographic anomaly. Such an anomaly is probably a good approximation to that produced by an island arc. This model relates the gravity anomaly directly

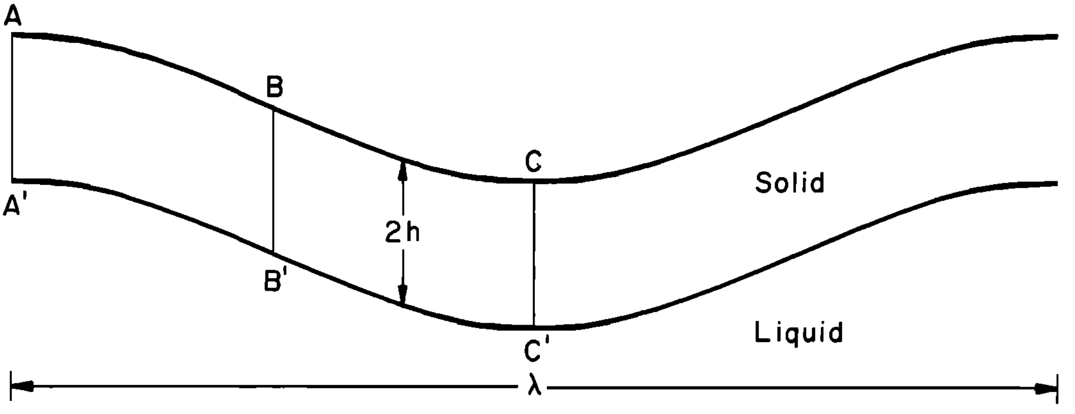

Fig. 5. The solid layer has density ρ and rigidity μ; the inviscid liquid half-space also has density ρ. Σ_2 is the dimensionless shear stress on AA′ and CC′; Σ_1, that on BB′. The deformation is exaggerated.

to the stress in the layer. Unfortunately, this relation is not unique since many different stress fields can produce the same anomaly. Despite this difficulty the solution can be used to estimate the stresses within the lithosphere and, hence, to decide the mechanism by which the anomalies are maintained.

A stressed solid may fail in extension or in shear, and either extension or shear may limit the magnitude of the surface deformation that the lithosphere can support. The strength of sea ice when surface loads are applied is a somewhat similar problem. *Weeks and Anderson* [1958] have demonstrated that failure occurs under loads about a factor of 3 greater than those predicted by elastic theory. Sea ice is, however, a partially molten solid and creeps easily under stress. It is therefore a poor model for the lithosphere, for which the elastic-plastic approximation should be reasonably accurate. There is also no reason to believe that the lithsphere fails in extension, as sea ice does when the bearing capacity is exceeded. Unless shear failure is dominant in trenches and island arcs, it is difficult to account for the first motion studies of shallow earthquakes in these areas [*Stauder and Bollinger*, 1966]. Fault plane solutions may be combined with aftershock distributions to demonstate that the islands are overthrusting the oceanic margins on low-angle thrust faults. Normal faults, which could be produced by failure in extension, are rare in such regions. Shear failure is therefore believed to be the more important process in the lithosphere.

The elastic equations for the displacement $\mathbf{u}$ in an incompressible solid are

$$\nabla \cdot \mathbf{u} = 0 \tag{22}$$

$$\frac{\mu}{\rho} \nabla^2 \mathbf{u} - g\mathbf{a}_z - \frac{1}{\rho} \nabla P = 0 \tag{23}$$

where $\mathbf{a}_z$ is a unit vector in the positive z direction. The boundary conditions for this model require the traction to vanish on the upper and lower deformed surfaces. If the deformation is small, this condition is approximately the same as requiring

$$\left[\frac{\partial u_x}{\partial z} + \frac{\partial u_z}{\partial x}\right]_{z=\pm h} = 0 \tag{24}$$

on the undeformed surfaces $z = \pm h$. If the normal stress on the upper deformed surface, $z = h(1 + \xi \cos kx)$ vanishes,

$$0 = P_{z=h(1+\xi \cos kx)} + 2\mu \left[\frac{\partial u_z}{\partial z}\right]_{z=h} \tag{25}$$

On the lower surface a similar equation results from the continuity of normal stress. The dimensionless equations can be obtained from (22) and (23) by substituting

$$z = hz'$$

$$x = hx'$$

$$P = gh\rho P'$$

$$\mathbf{u} = h\mathbf{u}'$$

$$k = 2\pi/\lambda = k'/h \tag{26}$$

to give

$$\nabla \cdot \mathbf{u}' = 0 \tag{27}$$

$$M\nabla^2\mathbf{u}' - \mathbf{a}_{z'} - \nabla P' = 0 \tag{28}$$

where

$$M = \mu/gh\rho \tag{29}$$

Since the problem is two dimensional, these equations are easily solved by using a potential ψ

$$\mathbf{u}' = \left(\frac{\partial\psi}{\partial z'}, 0, -\frac{\partial\psi}{\partial x'}\right) \tag{30}$$

Thus, (27) is satisfied for any ψ, and the curl of (28) requires

$$\nabla^4\psi = 0 \tag{31}$$

The solution to (31) of the form required is

$$\psi = \frac{\xi}{2Mk'^2}[(A + Bz')e^{k'z'} + (C + Dz')e^{-k'z'}] \sin k'x' \tag{32}$$

where A, B, C, and D are constants that must be determined from the boundary conditions. Substitution of (32) and (30) into (28) gives

$$P' = -\frac{\xi}{k'}(B\, e^{k'z'} + D\, e^{-k'z'}) \cdot \cos k'x' + 1 - z' \tag{33}$$

Then the boundary conditions (24) and (25) require

$$\begin{bmatrix} e^{k'}, & e^{k'}, & -e^{-k'}, & -e^{-k'} \\ e^{-k'}, & -e^{-k'}, & -e^{k'}, & e^{k'} \\ e^{k'}, & \left(\frac{1}{k'} + 1\right)e^{k'}, & e^{-k'}, & \left(-\frac{1}{k'} + 1\right)e^{-k'} \\ e^{-k'}, & \left(\frac{1}{k'} - 1\right)e^{-k'}, & e^{k'}, & -\left(\frac{1}{k'} + 1\right)e^{k'} \end{bmatrix} \begin{bmatrix} A \\ B \\ C \\ D \end{bmatrix} = \begin{bmatrix} 1 \\ 0 \\ 0 \\ 0 \end{bmatrix} \tag{34}$$

Inversion then determines the constants. The two-dimensional stress tensor can now be determined throughout the layer. For a given value of k' failure will occur where the shearing stress σ is greatest. The value of σ can be obtained by rotating the coordinate axes until the off-diagonal component of the stress tensor reaches a maximum:

$$\sigma(x, z) = \{[\sigma_{xz}(x, z)]^2 + [\sigma_{xx}(x, z)]^2\}^{1/2} \tag{35}$$

where

$$\begin{aligned} \sigma_{xx} &= -g\rho h\xi[F(z') - G(z')] \cos k'x' \\ \sigma_{xz} &= -g\rho h\xi[F(z') + G(z')] \sin k'x' \\ F(z') &= \left[A + B\left(z' + \frac{1}{k'}\right)\right]e^{k'z'} \\ G(z') &= \left[C + D\left(z' - \frac{1}{k'}\right)\right]e^{-k'z'} \end{aligned} \tag{36}$$

Thus,

$$\sigma = g\rho h\xi[F^2 + G^2 - 2FG \cos 2k'x']^{1/2} \tag{37}$$

For any value of z' stationary values of σ are

$$\frac{\sigma_1}{g\rho h\xi} = \Sigma_1 = |F + G| \tag{38}$$

at

$$k'x' = \frac{\pi}{2} + n\pi$$

and

$$\frac{\sigma_2}{g\rho h\xi} = \Sigma_2 = |F - G| \tag{39}$$

at

$$k'x' = m\pi$$

where n and m are integers. Whether

$$\Sigma_1 \lessgtr \Sigma_2$$

depends on the values of k' and z'. Σ_1 and Σ_2 for four values of k' in Figures 6 and 7 are simple when $k' \gg 1$ or $\ll 1$ and suggest asymptotic solutions will be good approximations in these ranges. When $k' \gg 1$, C and D can be neglected. Then

$$A = (k' + 1)e^{-k'} \qquad B = -k'e^{-k'} \tag{40}$$

hence,

$$\Sigma_1 = \Sigma_2 = k'(1 - z')e^{-k'(1-z')} \tag{41}$$

Thus, the maxima of both Σ_1 and Σ_2 are $1/e$ at $z' = 1 - (1/k')$. The asymptotic expressions when $k' \ll 1$ are more troublesome to obtain, since (34) must be solved in full. Also, it is necessary to retain terms through k'^3 in the expansion of the exponentials. The resulting expressions are

$$\Sigma_1 = \frac{3(1 - z'^2)}{4k'} \tag{42}$$

$$\Sigma_2 = \frac{3}{4k'^2}|z'| \tag{43}$$

Thus, the maximum value of the dimensionless shear stress Σ is

$$\Sigma = \frac{3}{4k'^2} \qquad k' \le 1$$
$$\Sigma = \frac{3}{4k'} \qquad k' \ge 1 \tag{44}$$

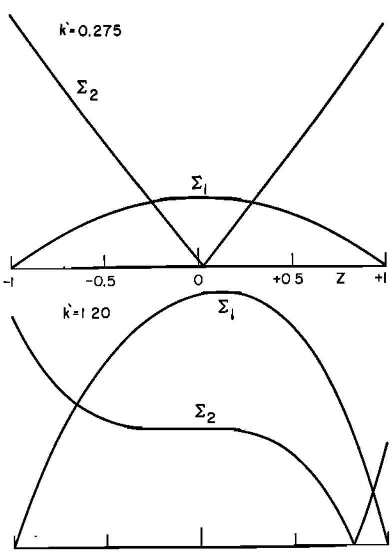

Fig. 6. Shear stresses for $k' = 0.275$ and 1.20.

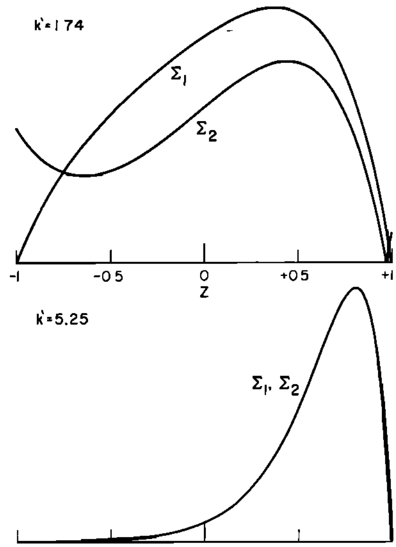

Fig. 7. Shear stresses for $k' = 1.74$ and 5.25.

The agreement between the asymptotic values of Σ and those determined numerically (Figure 8) is good for all values of k'. The maximum shear stress σ_{max} required to support a given deformation can, therefore, be estimated from (41) and (44):

$$\sigma_{max} = g\rho h\xi H(k') \tag{45}$$

where

$$H(k') = \frac{1}{e} \qquad k' > 2$$
$$= \frac{3}{4k'} \qquad 1 < k' < 2 \tag{46}$$
$$= \frac{3}{4k'^2} \qquad k' < 1$$

Failure in extension can occur whenever σ_{xx} has its greatest positive value. If $k' \gg 1$, σ_{xx} is negative everywhere, and therefore failure in extension cannot occur. However, when $k' \ll 1$,

$$\Sigma_{xx} = \frac{3}{2k'^2} \tag{47}$$

at

$$k'x' = (2m + 1)\pi \qquad z' = 1$$

Thus, failure could occur at the upper surface of the valleys. Since the solution for $\mathbf{u}'$ is not

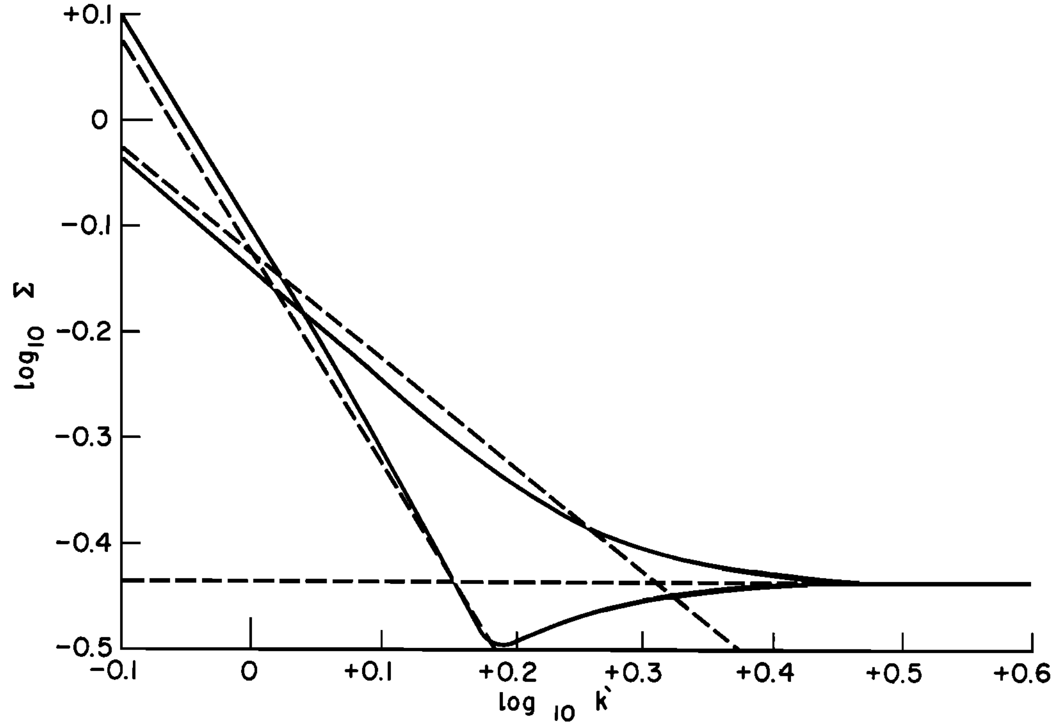

Fig. 8. A comparison between exact (solid line) and asymptotic (dashed line) solutions to (38) and (39) for maximum values of Σ_1 and Σ_2.

unique, this possibility can be removed by applying a compressive force

$$\Sigma_{xx} = -\frac{3}{2k'^2}$$

to the layer. The shear stress is then given by (45) and (46), except if $k' < 2$, when

$$H(k') = 3/2k'^2 \tag{48}$$

Since estimates of σ_{max} may well be in error by a factor of 2, this correction is neglected.

Jeffreys [1929] has obtained solutions to a problem that is similar to the one discussed here. He was interested in the stresses produced by mountains and solved the stress field within the floating layer when normal forces are applied to its upper surface. For $k' \gg 1$, his results agree with the results given here. For sufficiently small k', however, he obtained stresses that tend to zero as k'^2, whereas the stresses from (46) tend to infinity as $1/k'^2$. The reason for this difference is that surface loads are compensated in Jeffreys' model when their wavelength is long compared with the thickness of the layer, whereas in this problem no compensation is possible since the surface deformation, not the surface load, is given.

The gravity anomaly from the deformed layer is most easily obtained from Poisson's equation in two dimensions:

$$\nabla^2 U = -4\pi G\rho \qquad \text{inside} \tag{49}$$

$$\nabla^2 U = 0 \qquad \text{outside} \tag{50}$$

If the earth is assumed to have a constant density equal to that of the layer, (49) becomes

$$\nabla^2 U = -3g/a \tag{51}$$

where a is the radius of the earth. The boundary conditions are that U and ∇U are continuous on the deformed surface. To first order in ξ, they are satisfied if

inside

$$U = -\frac{3}{2}\frac{gh^2}{a}z'^2 - ghz' + \frac{3gh^2\xi}{2k'a}e^{k'z'}\cos k'x' \tag{52}$$

and outside

$$U = -ghz' + \frac{3gh^2\xi}{2k'a} e^{-k'z'} \cos k'x' \qquad (53)$$

where z' in (52) and (53) is measured from the undeformed upper surface.

Thus, the trough-to-peak amplitude of the free air gravity anomaly measured on a level surface with $z' = 0$ is

$$\Delta g = 3gh\xi/a \qquad (54)$$

Similarly, the trough-to-peak deformation of the geoid ΔG is

$$\Delta G = 3h^2\xi/k'a \qquad (55)$$

Substitution into (45) gives

$$\sigma_{\max} = \frac{\rho a \, \Delta g}{3} H(k') \qquad (56)$$

or

$$\sigma_{\max} = \frac{ga\rho \, \Delta G}{3h} k' H(k') \qquad (57)$$

The values of $\sigma_{\max}$ in Table 1 were obtained from (46), (56), and (57) with $g = 10^3$ cm/sec^2, $\rho = 3$ g/cc, and $a = 6 \times 10^8$ cm. The thickness of the layer is $2h$.

In experiments on dunite under a confining pressure of 5 kb *Griggs et al.* [1960] produced failure in shear at 800°C when $\sigma \simeq 4$ kb. Unfortunately, the loading rate in any laboratory experiment must be many orders of magnitude greater than that within the earth. It is probable that the failure stress under geological conditions is perhaps an order of magnitude smaller, since it would then be comparable with the stress release in large earthquakes [*Brune and Allen*, 1967]. For the purpose of this discussion the strength is taken to be 200 bars, though there is little justification for this choice.

The mid-continental gravity anomaly is given as a Bouguer anomaly by *Craddock et al.* [1963]. Since the topography is flat, the amplitude of the Bouguer and free air anomalies are approximately the same. Both this anomaly and the anomaly over the Hawaiian ridge can probably be supported by a lithosphere 50 km thick. This result agrees with the absence of earthquakes in both regions, except the earthquakes generated by basaltic magma movements beneath Hawaii [*Eaton*, 1962].

The gravity anomalies over the Puerto Rican and Tonga trenches require considerably larger stresses than Hawaii. If, however, the lithosphere is 100 km thick, rather than 50 km thick, in these regions, it may be able to support the anomalies for a limited time. Earthquakes would result when failure occurred, and therefore there must be some mechanism of regenerating the

TABLE 1

	λ, km	Δg, gals	k' when $2h = 50$ km	$\sigma_{\max}$, bars	k' when $2h = 100$ km	$\sigma_{\max}$, bars
Mid continent Gravity high *Craddock et al.* [1963]	80	0.1	2.0	22	3.9	22
Hawaiian ridge *Wollard* [1966]	140	0.3	1.1	120	2.2	67
Tonga *Talwani et al.* [1961] Puerto Rico *Talwani et al.* [1959]	300	0.5	0.52	830	1.0	220
		ΔG, meters				
Geoid	6,000	100	0.026	6.8×10^4	0.052	1.7×10^4
			k' when $2h = 3{,}000$ km			
Bulge	18,000	200	0.50	180		

stresses released by earthquakes. There is some evidence that the velocity and Q of the upper mantle is greater beneath trenches [*Oliver and Isacks*, 1967], and therefore the lithosphere may be thicker in these regions. These arguments show that the gravity anomalies over trenches cannot be proved to be supported by downward forces on the base of the lithosphere, and therefore they are not at present relevant to the problem of convection within the mantle.

It is fortunate that the trenches do not require normal stresses of $\sim 10^3$ bars on the base of the lithosphere, because present convection theories are not able to produce them. The normal stress produced by flow in a viscous fluid is given by

$$\sigma_{zz} = 2\eta \frac{\partial v_z}{\partial z} \simeq \frac{2\eta v}{d} \tag{58}$$

if

$$\begin{aligned} \eta &= 3 \times 10^{21} \text{ poise} \\ v &= 4 \text{ cm/yr} \\ d &= 5 \times 10^{7} \text{ cm} \end{aligned} \tag{59}$$

$$\sigma_{zz} \sim 15 \text{ bars}$$

If this estimate is incorrect by two orders of magnitude, fundamental changes are required in all existing theories of convection. At present there is no support for such profound changes. The same argument can be used to show that the convection currents are sufficient to regenerate the stresses involved in earthquakes. The traction exerted on the base of the lithosphere is ~ 10 bars. This stress acts everywhere between the ridges and the trenches, commonly a distance of ~ 2000 km and must be opposed by forces in the trench region acting within the lithosphere, ~ 100 km thick. Thus, the stresses are magnified by a factor of 20, to ~ 200 bars.

The deviations of the geoid from an oblate spheroid are ~ 100 meters. Table 1 clearly shows that they cannot be supported by the lithosphere. Such deviations must therefore be actively maintained by flow within the mantle and may be produced by small regional temperature differences [*McKenzie*, 1967*b*].

The last entry in Table 1 is included to compare the stress estimated in this simple manner from (57) with the stress of 163 bars obtained by *Kaula* [1963] for an elastic incompressible mantle. The agreement is considerably better than one would expect from the nature of the approximations involved.

Conclusion

These simple models for heat flow and gravity anomalies show that only the long-wavelength harmonics of the external gravity field must be maintained by mantle processes below the lithosphere. Therefore, any theory of convection within the mantle should be related to these observations and not to the geographic position of the ridges. Because of the deep earthquakes and not because of the gravity anomalies, trenches must also be related to the three-dimensional flow.

Acknowledgments. I would like to thank Dr. R. L. Parker and Dr. F. J. Vine for advice and encouragement and Dr. W. H. K. Lee for permission to reproduce Figures 2–4. I am also grateful to Sir Edward Bullard for suggesting several improvements to the argument.

This research was supported by the Air Force Office of Scientific Research, Office of Aerospace Research, United States Air Force, under AFOSR contract AF-49(638)-1337.

References

Brune, J. N., and C. R. Allen, A low-stress-drop low-magnitude earthquake with surface faulting: The Imperial, California earthquake of March 4, 1966, *Bull. Seismol. Soc. Am., 57,* 501–514, 1967.

Bullard, E. C., The flow of heat through the floor of the Atlantic Ocean, *Proc. Roy. Soc. London, A, 222,* 408–429, 1954.

Bullard, E. C., A. E. Maxwell, and R. Revelle, Heat flow through the deep sea floor, *Advan. Geophys, 3,* 153–181, 1956.

Craddock, C., E. C. Thiel, and B. Gross, A gravity investigation of the Precambrian of southeastern Minnesota and western Wisconsin, *J. Geophys. Res., 68,* 6015–6032, 1963.

Eaton, J. P., Crustal structure and volcanism in Hawaii, *Crust of the Pacific Basin, Geophys. Monograph 6,* pp. 13–29, American Geophysical Union, Washington, D. C., 1962.

Elder, J. W., Physical processes in geothermal areas, *Terrestrial Heat Flow, Geophys. Monograph 8,* pp. 211–239, American Geophysical Union, Washington, D. C., 1965.

Ewing, M., J. Brune, and J. Kuo, Surface-wave studies of the Pacific crust and mantle, *Crust of the Pacific Basin, Geophys. Monograph 6,* pp. 30–40, American Geophysical Union, Washington, D. C., 1962.

Fisher, O., *Physics of the Earth's Crust,* Macmillan, New York, 1889.

Fisher, R. L., and H. H. Hess, Trenches, in *The Sea*, vol. 3, edited by M. N. Hill, Interscience, New York, 1962.

Griggs, D. T., F. J. Turner, and H. C. Heard, Deformation of rocks at 500 to 800°C, *Am. Geol. Soc. Mem. 79*, chapter 4, 1960.

Jeffreys, H., *The Earth*, 2nd ed., Cambridge University Press, New York, 1929.

Kaula, W. M., Elastic models of the mantle corresponding to variations in the external gravity field, *J. Geophys. Res., 68*, 4967–4978, 1963.

Knopoff, L., S. Mueller, and W. L. Pilant, Structure of the crust and upper mantle in the Alps from the phase velocity of Rayleigh waves, *Bull. Seismol. Soc. Am., 56*, 1009–1044, 1966.

Langseth, M. G., X. Le Pichon, and M. Ewing, Crustal structure of the mid-ocean ridges, 5, Heat flow through the Atlantic Ocean floor and convection currents, *J. Geophys. Res., 71*, 5321–5355, 1966.

Lee, W. H. K., and S. Uyeda, Review of heat flow data, *Terrestrial Heat Flow, Geophys. Monograph 8*, pp. 87–190, American Geophysical Union, Washington, D. C., 1965.

McKenzie, D. P., The geophysical importance of high temperature creep, *Proc. NASA Conf. on History of Earth's Crust*, Princeton University Press, Princeton, N. J., in press, 1967*a*.

McKenzie, D. P., The Influence of the boundary conditions on convection in the earth's mantle, in press, *Geophys. J.*, 1967*b*.

Oliver, J., and B. L. Isacks, Some evidence on the structure of the mantle near island arcs (abstract), *Trans. Am. Geophys. Union, 48*, 219, 1967.

Runcorn, S. K., Changes in the convection pattern in the earth's mantle and continental drift: Evidence for a cold origin of the earth, *Phil. Trans. Roy. Soc., A, 258*, 228–251, 1965.

Stauder, W., and G. A. Bollinger, The focal mechanism of the Alaska earthquake of March 28, 1964, and its aftershock sequence, *J. Geophys. Res., 71*, 5283–5296, 1966.

Talwani, M., G. H. Sutton, and J. L. Worzel, A crustal section across the Puerto Rico trench, *J. Geophys. Res., 64*, 1545–1553, 1959.

Talwani, M., J. L. Worzel, and M. Ewing, Gravity anomalies and crustal structure across the Tonga trench, *J. Geophys. Res., 66*, 1265–1278, 1961.

Turcotte, D. L., and E. R. Oxburgh, Finite amplitude convective cells and continental drift, *J. Fluid Mech., 28*, 29–42, 1967.

Vacquier, V., and R. P. von Herzen, Evidence for connection between heat flow and the mid-Atlantic ridge magnetic anomaly, *J. Geophys. Res., 69*, 1093–1101, 1964.

Vine, F. J., and D. H. Matthews, Magnetic anomalies over ocean ridges, *Nature, 199*, 947–949, 1963.

Vine, F. J., Spreading of the ocean floor: New evidence, *Science, 154*, 1405–1415, 1966.

Weeks, W. F., and D. L. Anderson, An experimental study of strength of young sea ice, *Trans. Am. Geophys. Union, 39*, 641–647, 1958.

Wollard, G. P., Crust and mantle relations in the Hawaiian area, in *Continental Margins and Island Arcs, Paper* 66–15, Geological Survey of Canada, 1966.

(Received June 30, 1967.)